Ferromagnet/Superconductor Hybridization for Magnonic Applications

Igor A. Golovchanskiy, Nikolay N. Abramov, Vasily S. Stolyarov, Vitaly V. Bolginov, Valery V. Ryazanov, Alexander A. Golubov, and Alexey V. Ustinov*

In this work, a new hybridization of superconducting and ferromagnetic orders is demonstrated, promising for magnonics. By measuring the ferromagnetic and spin wave resonance absorption spectra of a magnetostatically coupled permalloy/niobium bilayer at different temperatures, magnetostatic spin wave resonances with unconventional dispersion are observed. The mechanism behind the modified dispersion, confirmed with micromagnetic simulations, implies screening of the alternating magnetostatic stray fields of precessing magnetic moments in the ferromagnetic layer by the superconducting surface in the Meissner state.

1. Introduction

Superconductivity (S) and ferromagnetism (F) are two antagonistic phenomena. Their coexistence attracts fundamental interest and promises a potential for applications, inaccessible for purely superconducting or ferromagnetic devices. Coexistence of ferromagnetism and superconductivity on atomic level in a bulk remains a rare phenomenon and have been observed fairly recently in complex compounds. The coexistence is mediated via the coupling of strong ferromagnetic order with triplet superconductivity,[1–3] or via orbital coupling of antiferromagnetic order with singlet superconductivity found in pnictides.[4,5]

The coexistence of ferromagnetism and superconductivity can be easily achieved in artificial superconductor/ferromagnet (S/F) hybrid structures, and involves a rich variety of approaches for such hybridization. The most obvious example for S/F hybridization is the compensation effect, which allows to reduce the actual magnetic field in S subsystem on macroscopic[6,7] or microscopic[8,9] scale by shielding it with F, and to modify the current–voltage characteristics of S.

On a microscopic scale, one basic direction studied intensively in last decades considers the proximity interaction between ferromagnetic and superconducting layers.[10,11] The proximity enables the Josephson coupling of superconducting electrodes via the ferromagnetic tunnel barrier with a possibility for π shift of the Josephson phase,[12,13] and allows to realize various superconducting spintronic elements,[14] including π-shifters for superconducting qubits[15] and logic blocks,[16] cryogenic memory elements,[17–19] F/S/F-like spin valves,[20–23] as well as more complex $0-\pi$ junction devices[24–26] and nanowires.[27]

Another basic direction for hybridization studied intensively in last decades considers the interaction of superconducting films, superconducting vortex matter in particular, with ferromagnetic sub-micro- or nanostructures.[11,28] In this case, the major physical effects revolve around manipulating the vortex media by means of the ferromagnetic nanostructures and sublattices and include the vortex matching effect[29,30] when the vortex lattice matches the lattice of ferromagnetic pinning centers, the vortex ratchet effect[29,31–33] when the asymmetric pinning potential of the ferromagnetic pinning center facilitates the preferable direction of vortex flow, and also vortex multiquanta states[34,35] and vortex-antivortex systems.[36,37]

Hybridization of a superconducting and ferromagnetic orders can also lead to the so-called domain wall superconductivity. Interaction of a superconducting layer with the

Dr. I. A. Golovchanskiy, Dr. V. S. Stolyarov, Prof. A. A. Golubov
Moscow Institute of Physics and Technology
State University
9 Institutskiy per., Dolgoprudny, Moscow Region 141700, Russia
E-mail: golov4anskiy@gmail.com

Dr. I. A. Golovchanskiy, N. N. Abramov, Dr. V. V. Bolginov, Prof. V. V. Ryazanov, Prof. A. V. Ustinov
National University of Science and Technology MISIS
4 Leninsky prosp., Moscow 119049, Russia

Dr. V. S. Stolyarov, Dr. V. V. Bolginov, Prof. V. V. Ryazanov
Institute of Solid State Physics (ISSP RAS)
Chernogolovka, Moscow Region 142432, Russia

The ORCID identification number(s) for the author(s) of this article can be found under https://doi.org/10.1002/adfm.201802375.

DOI: 10.1002/adfm.201802375

Dr. V. S. Stolyarov, Prof. V. V. Ryazanov
Solid State Physics Department
Kazan Federal University
Kazan 420008, Russia

Dr. V. V. Bolginov
Skobeltsyn Institute of Nuclear Physics
Lomonosov Moscow State University
Moscow 119991, Russia

Prof. A. A. Golubov
Faculty of Science and Technology and MESA+ Institute for Nanotechnology
University of Twente
Enschede 7500 AE, The Netherlands

Prof. A. V. Ustinov
Physikalisches Institut
Karlsruhe Institute of Technology
Karlsruhe 76131, Germany

domain structure enhances locally the superconducting order at the domain wall due to compensation of magnetostatic stray fields[38] or exchange fields.[39]

In a broader sense, hybridization also takes place for the dynamics of magnetic moment in the vicinity of superconducting subsystem. Such hybrid superconductor–ferromagnet systems found application in metamaterials where, according to Veselago criteria,[40] the superconducting layers provide the negative dielectric constant of a media, while the ferromagnetic layers ensures its negative magnetic permeability in vicinity of the ferromagnetic resonance, and the overall layered media is characterized by the negative refraction index.[41] Also, the magnetic moment can be coupled to the current oscillations in a hybrid Josephson junction[42–44] enabling additional ferromagnetic resonance modulated features on the Josephson current–voltage characteristics. At last, hybridization of magnons and microwave photons within superconducting circuits[45,46] can also be counted as the superconductor/ferromagnet hybrid system.

Reviewing briefly all sorts of superconducting/ferromagnetic hybrids we aim to emphasize that in the vast majority the "hybridization" implies modification of superconducting properties of films and structures. Alternatively, a number of reports on modification of ferromagnetic properties by hybridizing the ferromagnetic subsystem with superconducting one is very limited. In particular, recent study revealed a mechanism that allows the control of magnetic properties through the superconductivity in F/S/F trilayers.[47,48] Also, several works consider the effect of the hybridization on the ferromagnetic resonance spectra.[49–52] The S/F hybridization enables a shift of the ferromagnetic resonance frequency in Fe(Py)/YBCO[49] due to formation of a spin-glass-like phase at the S/F interface, or enhancement of the quality factor of the resonance in Py/Nb[50] due to spin pumping through the S/F interface.

In this work, we explore the S/F hybridization from a new angle, in terms of modification of ferromagnetic properties. Using a permalloy/niobium (Py/Nb) S/F bilayer, we demonstrate both experimentally and theoretically that the presence of a superconductor modifies heavily the spin wave dispersion of a ferromagnetic layer. This hybridization opens unexplored opportunities for tuning the spin-wave spectra of a ferromagnetic media for magnonic applications.[53–56]

2. Experimental Results and Discussion

Figure 1a shows the normalized transmission spectrum $S_{21}(f, H)$ of the Py/Nb bilayer sample, more specifically, of Py films placed on top of the transmission line of Nb coplanar waveguide (CPW), measured at $T = 4$ K, that is below the superconducting critical temperature T_c of Nb CPW, and at in-plane magnetic field H swept from 1.8×10^4 to -1.8×10^4 A m^{-1} (see Section 4 for details). The spectrum S_{21} was measured at the applied RF power

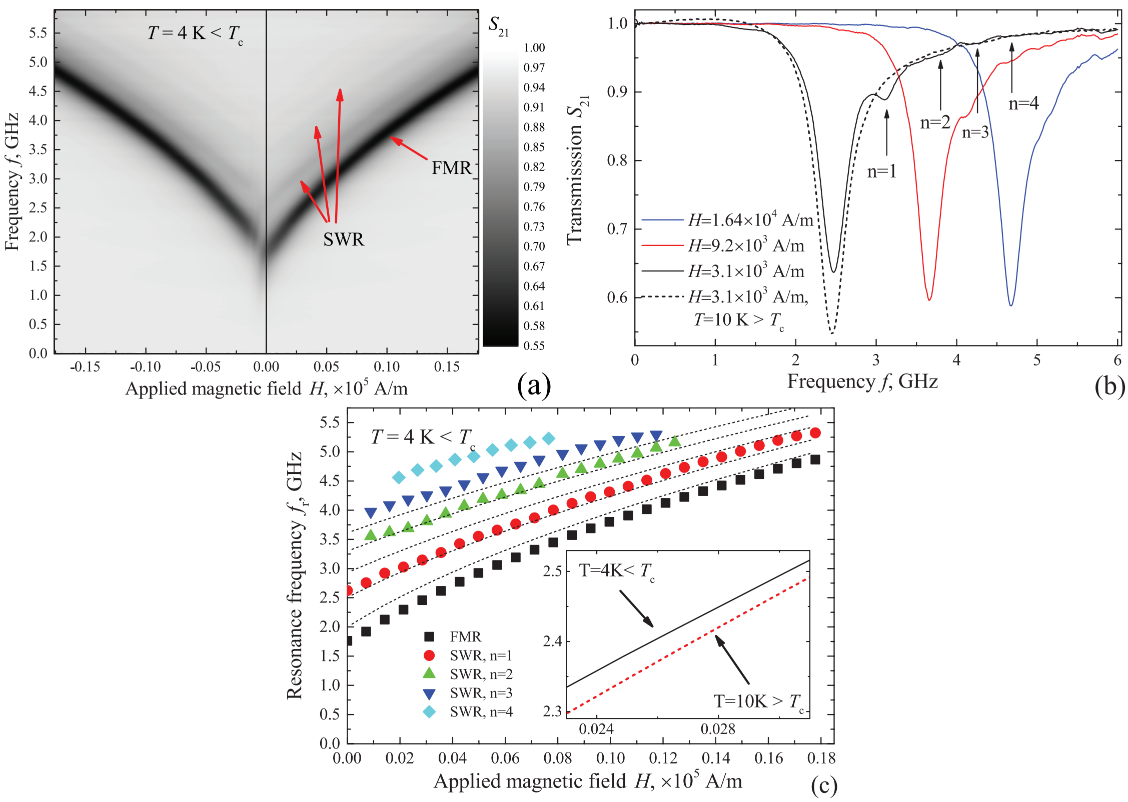

Figure 1. a) Gray-scale-coded absorption spectra in the frequency—field coordinates acquired for Py films at 4 K; b) dependencies of the S_{21} transmission on frequency f at several fixed applied magnetic fields H; c) dependencies of FMR and SWR frequencies f_r on applied magnetic field H extracted from (a). Dashed lines show the resonance curves $f_r(H)$ for conventional standing magnetostatic spin wave modes (Equation (2)) with the wavelength $(2n - 1)\lambda_n/2 = W = 130$ µm and $n = 1, 2, \ldots 5$).

0 dBm. In the experiment the power was ranged from −10 to 0 dBm and no dependence of the spectrum on the power was observed. At higher powers, >0 dBm, a heating of the sample occurred. Figure 1b shows several cross-sections of the spectrum at fixed magnetic fields H, i.e., $S_{21}(f)$. At $T < T_c$ the spectrum consists of a strong ferromagnetic resonance (FMR) absorption mode at lower frequencies and several additional weaker absorption modes at higher frequencies. The additional absorption modes manifest spin wave resonances and are indicated with arrows in Figure 1a,b. Point data in Figure 1c summarizes the experimental findings and shows dependencies of FMR and spin wave resonance (SWR) frequencies f_r on magnetic field H.

The key feature of absorption measurements in this work is an abrupt dependence of the SWR spectra on temperature. More specifically, SWR responses vanish completely when the absorption is measured at any $T > T_c$, where only the FMR response remains. This is depicted with $S_{21}(f)$ curve measured at $T = 10$ K in Figure 1b (shown with dashed line), which indicates the FMR absorption only and absence of any additional SWR modes. Also, the FMR at $T > T_c$ is observed at slightly lower frequencies (see the inset in Figure 1c).

The dependence of FMR frequency f_r on applied magnetic field H provides the effective anisotropy field (H_a) and the magnetization saturation (M_s) via the Kittel formula for thin films with in-plane magnetization in the absence of a perpendicular or surface anisotropy[57,58]

$$\left(2\pi f_r/\gamma\right)^2 = (H + H_a)(H + H_a + M_s) \tag{1}$$

where $\gamma = 2.21 \times 10^5$ mA^{-1}s^{-1} is the gyromagnetic ratio. The fits of FMR curves using Equation (1) yield the saturation magnetization $M_s \simeq 9.288 \times 10^5$ A m^{-1} and the anisotropy field $H_a \simeq 0.025 \times 10^5$ A m^{-1} at $T = 4$ K, and $M_s \simeq 9.359 \times 10^5$ A m^{-1} and the anisotropy field $H_a \simeq 0.023 \times 10^5$ A m^{-1} at $T = 10$ K. Thus, superconductivity of the CPW increases the FMR frequencies (the insert in Figure 1c) by enhancing the effective anisotropy H_a by ≈8%. In particular, at $H = 3.1 \times 10^3$ A m^{-1} it provides $f_r = 2.47$ GHz at $T < T_c$ and $f_r = 2.45$ GHz at $T > T_c$ (Figure 1b,c)

2.1. Identification of the Wave Nature

The SWR observed at $T < T_c$ (Figure 1) we define as the standing magnetostatic surface wave (MSSW) resonance absorption. A good overview on various magnetostatic spin wave modes is given in refs. [54,59,60]. Indeed, among three types of magnetostatic wave modes the forward volume mode can be observed when magnetic field is applied perpendicular to the film and, therefore, is prohibited by the geometry of the experiment. Excitation of the backward volume mode with a finite wave number at fixed magnetic field result in lower resonance frequency as compared to the FMR frequency, i.e., in opposite to the trend observed in Figure 1.

Technically, the perpendicular exchange standing spin waves (PSSW) can be considered.[54,61,62] Yet, in order to be coupled with uniform AC magnetic field the PSSW require either assymetric or symmetric closed boundary conditions, or substantially nonuniform magnetic properties across the thickness.[63] Otherwise, additional means for PSSW excitation are required.[64] In conventional VNA-FMR experiments with in-plane magnetic field the PSSW are not excited in Py thin films.

Thus, the MSSW is the only remaining explanation for SWR observed. The MSSW is observed with in-plane wave vector perpendicular to the direction of in-plane magnetic field and follows the dispersion relation[54,59,60,65]

$$\begin{aligned}\left(2\pi f_r/\gamma\right)^2 &= (H + H_a)(H + H_a + M_s)\\ &\quad + M_s^2\left(1 - \exp(-2kd)\right)/4\end{aligned} \tag{2}$$

where $k = 2\pi/\lambda$ is the wave vector. At the MSSW standing wave resonance the wave-length is quantized with the width of the F-sample W[59] with the closed symmetric boundary conditions. Dashed lines in Figure 1c show the conventional MSSW resonance curves with the resonant wave-length $(2n - 1)\lambda_n/2 = W = 130$ µm and $n = 1, 2, \ldots, 5$. The conventional MSSW resonances are at similar frequency range as the experimentally observed ones, which points towards the MSSW origin of the experimentally observed SWR. Yet, the resonance curves for conventional MSSW mismatch the experimentally observed ones, implying a heavy impact of superconductivity on a spin-wave dispersion relation.

2.2. Impact of Superconductivity: Micromagnetic Illustration

Summing up, the overall influence of the superconductivity of CPW on the dynamics of the F-layer is represented i) by higher effective anisotropy field H_a and, correspondingly, enhanced FMR frequency, and ii) by promotion of the standing MSSW resonance with unconventional dispersion.

We argue that the very basic phenomenon of superconductivity, namely, the perfect diamagnetism or the Meissner state, affects the dynamics of the F-layer. Indeed, a superconductor, being in a close proximity to precessing magnetic moments, screens the alternating magnetostatic stray fields and, in turn, affects the actual magnetic field acting on the magnetic moments. We believe the proper theoretical analysis of the magnetization dynamics of inductively coupled S/F hybrids will be carried out later. Here we illustrate the effect of superconducting (i.e., of perfect diamagnetic) response on magnetization dynamics of the F-layer using the micromagnetic simulations.[66,67]

The magnetostatic problem of a S/F hybrid structure can be treated as magnetostatic interaction of two ferromagnets with micromagnetic simulations in two convenient ways. The one way, applicable in general for a finite size superconducting object in external magnetic field H, including magnetostatic stray fields of a ferromagnet in vicinity, implies zeroing out the magnetic flux $\vec{B}(\vec{r}_S)$ everywhere inside the superconductor, i.e., setting $\vec{M}_S(\vec{r}_S) \propto -\vec{H}(\vec{r}_S)$, where $\vec{r}_S$ is a position inside the finite superconductor. Then, the magnetostatic interaction of the F with S is equivalent to the interaction of the F with $\vec{M}_S(\vec{r}_S)$. The second approach, used in this work, is referred commonly as the method of images, and is applicable for a finite F-layer placed in vicinity to an infinite superconducting surface. The method of images, illustrated in Figure 3a, implies magnetostaic interaction of magnetic moments of the F $\vec{M}(x, y, z) = (M_x, M_y, M_z)$ located over a distance z above the superconducting surface $x - y$ with the mirror image moments $\vec{M}_{im}(x, y, -z) = (M_x, M_y, -M_z)$. We note here that for thin film

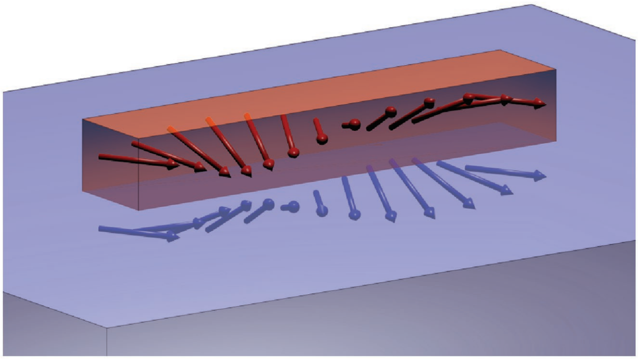

Figure 2. Illustration of the method of images. A finite-size ferromagnet (shown in red) is placed on the surface of a superconductor (shown in blue). The superconductor, as an ideal diamagnet, excludes the magnetostaic stray fields of the ferromagnet. Within micromagnetic terms such coupling is equivalent to interaction of ferromagnetic spins (red arrows) the their mirrored image in respect to the superconducting surface (blue arrows).

geometries the perfect diamagnetism of a superconductor and its micromagnetic representation are valid at any orientation of in-plane magnetic fields. The case of out-of-plane external magnetic field is more complicated, and a possibility for screening of the alternating magnetostatic stray fields in out-of-plane geometry is not apparent. In particular, the magnetic field penetrates into type II superconducting film with vortices, $B \approx H$ in the superconductor, and, therefore, no macroscopic screening is present. Yet, the Meissner screening currents remain.

To capture the magnetization dynamics activity influenced by the perfect diamagnetism of superconducting layer, we perform a dynamic micromagnetic simulation on a $X \times Y \times Z$ $130 \times 130 \times 0.09$ μm^3 Py film with $M_s = 9.3 \times 10^5$ A m^{-1}, $H_a = 2.5 \times 10^3$ A m^{-1} and Gilbert damping $\alpha = 0.01$ employing a 1D $1 \times 1300 \times 1$ mesh along y-axis with $130 \times 0.1 \times 0.09$ μm^3 cells, following ref. [65]. In the numerical experiment we apply a constant magnetic field $H = 3.1 \times 10^3$ A m^{-1} along x, a small AC magnetic field along y direction, and derive the dependence of the averaged amplitude of the steady state magnetization precession on frequency f of AC field. The frequency of maximum amplitude corresponds to the maximum energy absorption from microwave (MW) field source.

First, we simulate the MW response of the F-layer in absence of superconducting screening (red line in Figure 3a), representing the experiment at $T > T_c$. The simulated MW response consists of the main absorption peak at $f = 2.60$ GHz, and multiple weaker resonance peaks that form a wavy pattern of absorption at f higher than the FMR frequency. Importantly, the main peak represents an intermediate Kittel-$\lambda/2$ MSSW resonance rather than a pure coherent Kittel FMR mode. The weaker peaks manifest the conventional standing MSSW resonance with the resonant wavelength $(2n + 1)\lambda_n/2 = W = 130$ μm and $n = 1, 2, ..., 8$ at frequency range $2.6 < f < 5.2$ GHz, with the first SWR mode corresponding to $W = 3\lambda_1/2$.

Next, we simulate the MW response of the F-layer placed on top of ideal superconducting surface, as shown in **Figure 2**, which represents the experiment at $T < T_c$. The MW response of such S/F hybrid is shown in **Figure 3**a with the black line. The simulated MW response consists of the same main absorption peak at $f = 2.68$ GHz, i.e., by 0.08 GHz higher than one at $T > T_c$. This correlates qualitatively with the experiment, where the same shift by 0.02 GHz was observed. Also, just as in experiment (Figure 1b), 4 additional distinct SWR peaks are observed, indicated with arrows. These are unconventional standing MSSW resonances with the same resonant wavelength $(2n + 1)\lambda_n/2 = W = 130$ μm and $n = 1, 2, ..., 4$ at frequency range $2.6 < f < 5.2$ GHz (the first SWR mode also corresponds to $W = 3\lambda_1/2$). Overall, the simulated spectrum matches qualitatively the experimental $S_{21}(f)$ at $H = 3.1 \times 10^3$ A m^{-1} (Figure 1b) with a well distinguishable $n = 1$ SWR mode, indicating that the perfect diamagnetism of Nb superconducting CPW is responsible for the observed SWR spectrum.

To compare experimental results with simulations quantitatively, Figure 3b shows the resonance frequency difference between the SWR mode and the FMR mode $\Delta f_r = f_{SWR} - f_{FMR}$ as a function of the mode number n at $H = 3.1 \times 10^3$ A m^{-1}. Figure 3b indicates a reasonable quantitative match of experimental $\Delta f_r(n)$ with one simulated for S/F bilayered structure, indicating the perfect diamagnetism as a valid approximation. Moreover, Figure 3b demonstrates a modification of the MSSW dispersion by the superconducting screening as follows. For standing waves the mode number is proportional to the wave vector $n \propto k$, therefore $\Delta f_r/n$ indicates the MSSW phase velocity, which is approximately by factor of 1.5 higher in presence of the screening than in absence of one. Thus, we confirm explicitly that the superconductor in the S/F hybrid modifies properties of the ferromagnet as the magnonic media.

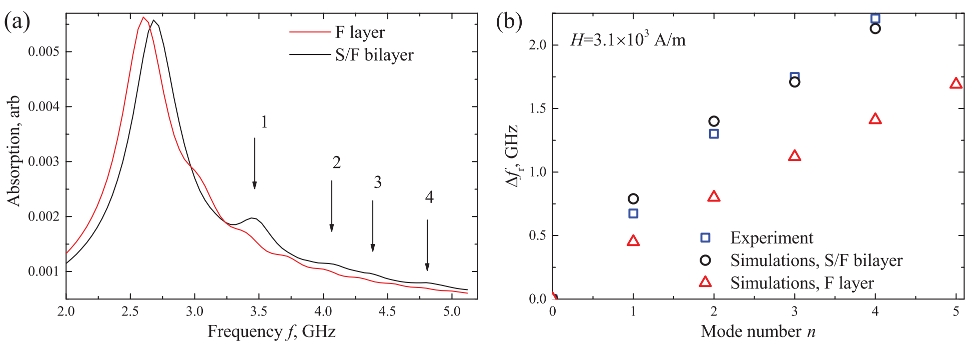

Figure 3. a) Simulated dependence of the amplitude of magnetization precession on frequency at $H = 3.1 \times 10^3$ A m^{-1}. b) Dependencies of difference between the FMR frequency and the SWR frequency Δf_r on the mode number n at $H = 3.1 \times 10^3$ A m^{-1}.

One last issue is required to be addressed. The superconductivity mediated MSSW resonances are well observed both experimentally and theoretically when the CPW is in superconducting state (Figures 1 and 3a, respectively), and also conventional MSSW resonances are observed theoretically when the CPW is in normal state (Figure 3a). Yet, the MSSW resonances are absent when the spectra is measured at $T > T_c$ (Figure 1b). In other terms, experimentally the coupling of the waveguide to the MSSW is much stronger at $T < T_c$. A reasonable qualitative explanation implies different distributions of the microwave currents across the CPW transmission line and, correspondingly, different distribution of the excitation AC magnetic field in ferromagnetic sample when measured above and below T_c. When the spectrum is measured at $T < T_c$ of Nb, the microwave currents are confined at the lateral edges of the CPW, within the distance of several λ_L, i.e., far from the edges of ferromagnetic sample. In this case the AC magnetic field is highly inhomogeneous in vicinity to the edges of CPW but remain homogeneous across the CPW in the F volume. Therefore, approximation of the uniform AC magnetic field in F volume, used for simulations, is valid. Alternatively, when the spectrum is measured at normal resistive state of Nb, the microwave currents are distributed more uniformly, resulting in a highly nonuniform distribution of AC magnetic field across the CPW in the F volume.[73] In this case, the AC magnetic field is maximum at the edges of the F, which violates the closed boundary conditions for MSSW standing wave. Since the closed boundary conditions are violated, the MSSW resonance is not excited in the experiment at $T > T_c$.

As a final remark we note that the effect of superconducting screening on magnetization dynamics in the ferromagnetic film resembles one of conducting nonmagnetic layers. Despite a fundamental difference between the superconducting Meissner effect and the perfect conductivity, eddy currents induced in a perfect conductor coupled inductively with a ferromagnetic film also shield the alternating magnetostatic stray fields and, in turn, affect the actual magnetic field acting on the magnetic moments in a similar manner.[68–72] However, real conductors are efficient in a limited length-scales, and affect spin waves with the length above the length of skin depth,[72] which is in micrometer range at microwave frequencies. In contrast, the wavelength of a spin wave for superconducting screening is limited by the London penetration depth, which is typically in the range of 10–100 nm for different superconductors and temperatures, offering applicability of superconductors in a broad range of spin wave frequencies/wavelengths, up to the range of exchange spin waves.

3. Conclusion

Summarizing, in this work we have studied the influence of superconductivity on magnetization dynamics of the ferromagnetic rectangular film deposited on top of the superconducting Nb waveguide. Measuring the microwave absorption spectrum at temperatures above and below the superconducting critical temperature we have shown that the superconductivity enhances marginally the ferromagnetic resonance frequency, and promotes standing magnetostatic surface spin wave resonances with unconventional dispersion relation. Using micromagnetic simulations combined with the method of images we have shown explicitly that the essence of the impact of superconductivity lies in perfect diamagnetic (Meissner) screening of magnetostatic stray fields of the ferromagnet by the superconducting surface. Presence of a superconducting surface in vicinity of a ferromagnet modifies heavily the spin-wave dispersion. In our particular experiment the phase velocity of MSSW is increased by a factor of 1.5.

The conventional magnetostatic waves in thin films obey the dispersion relation $f = f(k, H, F, d_F)$, where k is the wave number, F implies magnetic properties of the ferromagnetic film (H_a, M_s, etc.), d_F is the thickness of the film. Placed on the superconducting surface, the magnetostatic waves in the F-layer start to obey an extended dispersion relation $f = f(k, H, F, d_F, \lambda_L, S, d_{S-F})$, which should include additionally the screening properties of superconductor, such as the London penetration depth λ_L, geometry of the superconductor indicated as S, and also distance between the F and S layers d_{S-F}. Proper consideration of the S and F properties gives unique opportunities for tuning the spin-wave dispersion for particular applications, and also implies additional temperature dependence of the dispersion relation modulated by superconducting properties.

4. Experimental Section

In this work, an influence of superconductivity on magnetization dynamics in F layer was studied measuring the FMR and SWR absorption spectra. The FMR and SWR absorption measurements were performed using the so-called VNA-FMR approach.[57,73] A schematic illustration of the experiment, including the sample design, is shown in **Figure 4**. The studied permalloy F sample (shown in red) in the form of a series of 1100 × 130 µm^2 rectangle films of thickness 90 nm and 200 µm spacing in-between was deposited on the central stripe of the superconducting Nb CPW formed on Si substrate. The 50 Ω impedance Nb CPW with 85–150–85 µm gap–center–gap size was patterned out of 150 nm thick Nb film with superconducting critical temperature

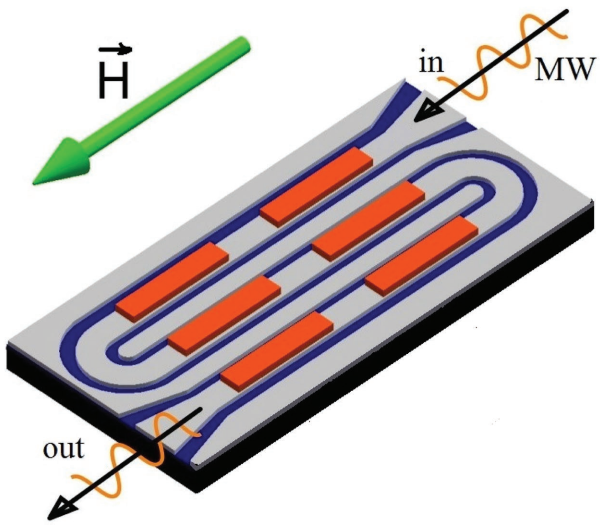

Figure 4. Schematic illustration of the sample design for FMR measurements. Patterned Py films (in red) are placed onto a 50 Ω coplanar waveguide made of Nb (in gray); insulating gaps of the waveguide are shown in blue. Black and green arrows show, respectively, the direction of propagation of the guided microwave and the direction of the external magnetic field (see details in the text).

$T_c \gtrsim 9$ K. The design of the test-chip ensures the limit of infinite thin film, and also the uniformity of the excitation AC-field in the F.[73] Bias magnetic field (green arrow in Figure 4) is oriented in-plane and parallel to the direction of the MW propagation, i.e., perpendicular to the AC field. The F sample couples to the AC magnetic field of the CPW and causes resonant losses and phase shift at FMR or SWR frequency. In this work, the same experimental setup was used for investigation of the resonant absorption as in ref. [74]. The setup enables measuring the ferromagnetic response at different temperatures 1.2–50 K and magnetic fields up to 1 T. The response of the system was studied by analyzing the transmitted MW signal S_{21} by vector network analyzer (VNA) Rohde&Schwarz ZVB20.

Nb CPW was fabricated using laser lithography and plasma-chemical etching technique in CF_4+O_2 out of Nb film magnetron sputtered onto Si substrate. Py thin film sample of ≈90 nm thickness was deposited directly onto Nb CPW using argon RF-sputtering of NiFe alloy target and double-resist lift-off technique. During the deposition the argon pressure and deposition rate were 1.5×10^{-2} mbar and 1.5 Å s^{-1}, respectively. The base pressure in the growth chamber prior deposition was 2×10^{-6} mbar. A 5 nm AlO_x insulating layer was deposited between the superconducting and the ferromagnetic layers to avoid the superconducting proximity effect.

Acknowledgements

This work was supported by the Ministry of Education and Science of the Russian Federation (Megagrant project No. 14.Y26.31.0007 and Research projects No. K2-2014-025 and No. K2-2016-051 in the framework of Increase Competitiveness Program of NUST "MISiS") and by the Russian Foundation for Basic Research (RFBR) (Research projects No. 16-02-00418 and No. 17-02-01270). V.S.S. and V.V.R. acknowledge the partial support by the Program of Competitive Growth of Kazan Federal University.

Conflict of Interest

The authors declare no conflict of interest.

Keywords

ferromagnetic resonance, magnonics, spin waves, superconductor/ferromagnet hybrids, superconducting Meissner state

Received: April 7, 2018
Revised: May 8, 2018
Published online: June 22, 2018

[1] S. S. Saxena, P. Agarwal, K. Ahilan, F. M. Grosche, R. K. W. Haselwimmer, M. J. Steiner, E. Pugh, I. R. Walker, S. R. Julian, P. Monthoux, G. G. Lonzarich, A. Huxley, I. Sheikin, D. Braithwaite, J. Flouquet, *Nature* **2000**, *406*, 587.
[2] D. Aoki, J. Flouquet, *J. Phys. Soc. Jpn.* **2012**, *81*, 011003.
[3] G. S. Thakur, G. Fuchs, K. Nenkov, Z. Haque, L. C. Gupta, A. K. Ganguli, *Sci. Rep.* **2016**, *6*, 37527.
[4] S. Nandi, W. T. Jin, Y. Xiao, Y. Su, S. Price, D. K. Shukla, J. Strempfer, H. S. Jeevan, P. Gegenwart, Th. Bruckel, *Phys. Rev. B* **2014**, *89*, 014512.
[5] V. S. Stolyarov, I. S. Veshchunov, S. Yu Grebenchuk, D. S. Baranov, I. A. Golovchanskiy, A. G. Shishkin, N. Zhou, Z. X. Shi, X. F. Xu, S. Pyon, Y. Sun, W. Jiao, G. Cao, L. Ya Vinnikov, A. A. Golubov, T. Tamegai, A. I. Buzdin, D. Roditchev, *Sci. Adv.* **2018**, https://doi.org/10.1126/sciadv.aat1016.
[6] Y. A. Genenko, A. Usoskin, H. C. Freyhardt, *Phys. Rev. Lett.* **1999**, *83*, 3045.
[7] A. V. Pan, S. X. Dou, *J. Appl. Phys.* **2004**, *96*, 1146.
[8] M. Lange, M. J. Van Bael, Y. Bruynseraede, V. V. Moshchalkov, *Phys. Rev. Lett.* **2003**, *90*, 197006.
[9] S. Haindl, M. Weisheit, T. Thersleff, L. Schultz, B. Holzapfel, *Supercond. Sci. Technol.* **2007**, *21*, 045017.
[10] A. I. Buzdin, *Rev. Mod. Phys.* **2005**, *77*, 935.
[11] I. F. Lyuksyutov, V. L. Pokrovsky, *Adv. Phys.* **2005**, *54*, 67.
[12] V. V. Ryazanov, V. A. Oboznov, A. Y. Rusanov, A. V. Veretennikov, A. A. Golubov, J. Aarts, *Phys. Rev. Lett.* **2001**, *86*, 2427.
[13] A. A. Golubov, M. Y. Kupriyanov, E. Ilichev, *Rev. Mod. Phys.* **2004**, *76*, 411.
[14] J. Linder, J. W. A. Robinson, *Nat. Phys.* **2015**, *11*, 307.
[15] A. K. Feofanov, V. A. Oboznov, V. V. Bolginov, J. Lisenfeld, S. Poletto, V. V. Ryazanov, A. N. Rossolenko, M. Khabipov, D. Balashov, A. B. Zorin, P. N. Dmitriev, V. P. Koshelets, A. V. Ustinov, *Nat. Phys.* **2010**, *6*, 593.
[16] A. V. Ustinov, V. K. Kaplunenko, *J. Appl. Phys.* **2003**, *94*, 5405.
[17] I. V. Vernik, V. V. Bol'ginov, S. V. Bakurskiy, A. A. Golubov, M. Y. Kupriyanov, V. V. Ryazanov, O. Mukhanov, *IEEE Trans. Appl. Supercond.* **2013**, *23*, 1701208.
[18] S. V. Bakurskiy, N. V. Klenov, I. I. Soloviev, V. V. Bol'ginov, V. V. Ryazanov, I. V. Vernik, O. A. Mukhanov, M. Kupriyanov, A. A. Golubov, *Appl. Phys. Lett.* **2013**, *102*, 192603.
[19] I. A. Golovchanskiy, V. V. Bolginov, V. S. Stolyarov, N. N. Abramov, A. B. Hamida, O. V. Emelyanova, B. S. Stolyarov, M. Y. Kupriyanov, A. A. Golubov, V. V. Ryazanov, *Phys. Rev. B* **2016**, *94*, 214514.
[20] L. R. Tagirov, *Phys. Rev. Lett.* **1999**, *83*, 2058.
[21] J. Gu, C.-Y. You, J. S. Jiang, J. Pearson, Y. B. Bazaliy, S. D. Baden, *Phys. Rev. Lett.* **2002**, *89*, 267001.
[22] D. Stamopoulos, E. Aristomenopoulou, *Sci. Rep.* **2015**, *5*, 13420.
[23] R. R. Gaifullin, R. G. Deminov, L. R. Tagirov, M. Yu. Kupriyanov, A. A. Golubov, *Physics of the Solid State* **2017**, *59*, 2114.
[24] E. C. Gingrich, B. M. Niedzielski, J. A. Glick, Y. Wang, D. L. Miller, R. Loloee, W. P. Pratt Jr., N. O. Birge, *Nat. Phys.* **2016**, *12*, 564.
[25] M. Weides, M. Kemmler, H. Kohlstedt, R. Waser, D. Koelle, R. Kleiner, E. Goldobin, *Phys. Rev. Lett.* **2006**, *97*, 247001.
[26] S. V. Bakurskiy, V. I. Filippov, V. I. Ruzhickiy, N. V. Klenov, I. I. Soloviev, M. Yu. Kupriyanov, A. A. Golubov, *Phys. Rev. B* **2017**, *95*, 094522.
[27] J. Wang, M. Singh, M. Tian, N. Kumar, B. Liu, C. Shi, J. K. Jain, N. Samarth, T. E. Mallouk, M. H. W. Chan, *Nat. Phys.* **2010**, *6*, 389.
[28] A. Y. Aladyshkin, A. V. Silhanek, W. Gillijns, V. V. Moshchalkov, *Supercond. Sci. Technol.* **2009**, *22*, 053001.
[29] J. E. Villegas, S. Savel'ev, F. Nori, E. M. Gonzalez, J. V. Anguita, R. García, J. L. Vicent, *Science* **2003**, *302*, 1188.
[30] M. Vélez, J. I. Martín, J. E. Villegas, A. Hoffmann, E. M. González, J. L. Vicent, I. K. Schuller, *J. Magn. Magn. Mater.* **2008**, *320*, 2547.
[31] C. C. de Souza Silva, A. V. Silhanek, J. V. de Vondel, W. Gillijns, V. Metlushko, B. Ilic, V. V. Moshchalkov, *Phys. Rev. Lett.* **2007**, *98*, 117005.
[32] D. P. de Lara, M. Erekhinsky, E. M. Gonzalez, Y. J. Rosen, I. K. Schuller, J. L. Vicent, *Phys. Rev. B* **2011**, *83*, 174507.
[33] A. Gomez, E. M. Gonzalez, M. Iglesias, N. Sanchez, F. J. Palomares, F. Cebollada, J. M. Gonzalez, J. L. Vicent, *J. Phys. D: Appl. Phys.* **2013**, *46*, 095302.
[34] C. Carballeira, V. V. Moshchalkov, L. F. Chibotaru, A. Ceulemans, *Phys. Rev. Lett.* **2005**, *95*, 237003.
[35] Q. H. Chen, C. Carballeira, V. V. Moshchalkov, *Phys. Rev. B* **2009**, *79*, 104520.
[36] M. Lange, M. J. V. Bael, A. V. Silhanek, V. V. Moshchalkov, *Phys. Rev. B* **2005**, *72*, 052507.
[37] C. L. S. Lima, C. C. de Souza Silva, *Phys. Rev. B* **2009**, *80*, 054514.
[38] Z. Yang, M. Lange, A. V., R. Szymczak, V. V. Moshchalkov, *Nat. Mater.* **2004**, *3*, 793.

[39] A. Rusanov, M. Hesselberth, J. Aarts, A. I. Buzdin, *Phys. Rev. Lett.* **2004**, *93*, 057002.
[40] V. G. Veselago, *Sov. Phys. Usp.* **1968**, *10*, 509.
[41] A. Pimenov, A. Loidl, P. Przyslupski, B. Dabrowski, *Phys. Rev. Lett.* **2005**, *95*, 247009.
[42] S. E. Barnes, M. Aprili, I. Petkovic, S. Maekawa, *Supercond. Sci. Technol.* **2011**, *24*, 024020.
[43] S. Mai, E. Kandelaki, A. F. Volkov, K. B. Efetov, *Phys. Rev. B* **2011**, *84*, 144519.
[44] I. A. Golovchanskiy, N. N. Abramov, V. S. Stolyarov, O. V. Emelyanova, A. A. Golubov, A. V. Ustinov, V. V. Ryazanov, *Supercond. Sci. Technol.* **2017**, *30*, 054005.
[45] H. Huebl, C. W. Zollitsch, J. Lotze, F. Hocke, M. Greifenstein, A. Marx, R. Gross, S. T. B. Goennenwein, *Phys. Rev. Lett.* **2013**, *111*, 127003.
[46] I. A. Golovchanskiy, N. N. Abramov, V. S. Stolyarov, I. V. Shchetinin, P. S. Dzhumaev, A. S. Averkin, S. N. Kozlov, A. A. Golubov, V. V. Ryazanov, A. V. Ustinov, *J. Appl. Phys.* **2018**, *123*, 173904.
[47] Y. Zhu, A. Pal, M. G. Blamire, Z. H. Barber, *Nat. Mater.* **2017**, *16*, 195.
[48] A. A. Golubov, M. Y. Kupriyanov, *Nat. Mater.* **2017**, *16*, 156.
[49] M. Rubinstein, P. Lubitz, W. E. Carlos, P. R. Broussard, D. B. Chrisey, J. Horwitz, J. J. Krebs, *Phys. Rev. B* **1993**, *47*, 15350.
[50] C. Bell, S. Milikisyants, M. Huber, J. Aarts, *Phys. Rev. Lett.* **2008**, *100*, 047002.
[51] O. A. Chivileva, A. G. Gurevich, I. A. Lineichuk, S. G. Shul'man, S. O. Fregatov, *Tech. Phys. Lett.* **2000**, *26*, 949.
[52] T. Muhge, N. N. Garif'yanov, Y. Goryunov, K. Theis-Brohl, K. Westerholt, I. A. Garifullin, H. Zabel, *Physica C* **1998**, *296*, 325.
[53] *Magnonics: From Fundamentals to Applications* (Eds: S. O. Demokritov, A. N. Slavin), Springer-Verlag, Berlin/Heidelberg **2013**.
[54] D. Stancil, *Theory of Magnetostatic Waves*, Springer-Verlag, New York, Inc. **1993**.
[55] V. V. Kruglyak, S. O. Demokritov, D. Grundler, *J. Phys. D: Appl. Phys.* **2010**, *43*, 264001.
[56] A. V. Chumak, A. A. Serga, B. Hillebrands, *J. Phys. D: Appl. Phys.* **2017**, *50*, 244001.
[57] Y.-C. Chen, D.-S. Hung, Y.-D. Yao, S.-F. Lee, H.-P. Ji, C. Yu, *J. Appl. Phys.* **2007**, *101*, 09C104.
[58] N. Alvarez, G. Alejandro, J. Gomez, E. Goovaerts, A. Butera, *J. Phys. D: Appl. Phys.* **2013**, *46*, 505001.
[59] C. Bayer, J. Jorzick, B. Hillebrands, S. O. Demokritov, A. N. Slavin, N. Gorn, M. P. Kostylev, *Spin Dynamics in Confined Magnetic Structures III*, Springer, Berlin/Heidelberg **2006**, pp. 57–103.
[60] A. A. Serga, A. V. Chumak, B. Hillebrands, *J. Phys. D: Appl. Phys.* **2010**, *43*, 264002.
[61] C. Kittel, *Phys. Rev.* **1958**, *100*, 1295.
[62] M. H. Seavey, P. E. Tannenwald, *J. Appl. Phys.* **1959**, *30*, S227.
[63] T. G. Rappoport, P. Redliński, X. Liu, G. Zaránd, J. K. Furdyna, B. Jankó, *Phys. Rev. B* **2004**, *69*, 125213.
[64] Y. V. Khivintsev, L. Reisman, J. Lovejoy, R. Adam, C. M. Schneider, R. E. Camley, Z. J. Celinski, *J. Appl. Phys.* **2010**, *108*, 023907.
[65] P. Deorani, J. H. Kwon, H. Yang, *Curr. Appl. Phys.* **2014**, *14*, S129.
[66] M. Donahue, D. Porter, *OOMMF User's Guide*, Version 1.0, Interagency Report NISTIR 6376, National Institute of Standards and Technology, Gaithersburg, MD **1999**.
[67] J. E. Miltat, M. J. Donahue, *Handbook of Magnetism and Advanced Magnetic Materials*, Vol. *2*, JohnWiley & Sons, Ltd. **2007**.
[68] K. Kawasaki, H. Takagi, M. Umeno, *IEEE Trans. Microwave Theory Tech.* **1974**, *22*, 924.
[69] T. Yukawa, J. Ikenoue, J. Yamada, K. Abe, *J. Appl. Phys.* **1978**, *49*, 376.
[70] M. Vroubel, B. Rejaei, *J. Appl. Phys.* **2008**, *103*, 114906.
[71] I. S. Maksymov, M. Kostylev, *J. Appl. Phys.* **2013**, *113*, 043927.
[72] M. Mruczkiewicz, M. Krawczyk, *J. Appl. Phys.* **2014**, *115*, 113909.
[73] I. Neudecker, G. Woltersdorf, B. Heinrich, T. Okuno, G. Gubbiotti, C. Back, *J. Magn. Magn. Mater.* **2006**, *307*, 148.
[74] I. A. Golovchanskiy, V. V. Bolginov, N. N. Abramov, V. S. Stolyarov, A. B. Hamida, V. I. Chichkov, D. Roditchev, V. V. Ryazanov, *J. Appl. Phys.* **2016**, *120*, 163902.